

The Value of Information in Human-AI Decision-making

Ziyang Guo*

Yifan Wu†

Jason Hartline‡

Jessica Hullman§

April 17, 2025

Abstract

Multiple agents—including humans and AI models—are often paired on decision tasks with the expectation of achieving *complementary performance*, where the combined performance of both agents outperforms either one alone. However, knowing how to improve the performance of a human-AI team is often difficult without knowing more about what particular information and strategies each agent employs. We provide a decision-theoretic framework for characterizing the value of information—and consequently, opportunities for agents to better exploit available information—in AI-assisted decision workflows. We demonstrate the use of the framework for model selection, empirical evaluation of human-AI performance, and explanation design. We propose a novel information-based explanation technique that adapts SHAP, a saliency-based explanation to explain information value in decision making.

1 Introduction

As the performance of artificial intelligence (AI) for domain-specific predictions improves, workflows in which human and AI models are combined to make decisions in medicine, finance, and law, among other domains. Often, statistical models can be developed that exceed the accuracy of human experts on average [Ægisdóttir et al., 2006, Grove et al., 2000, Meehl, 1954]. However, whenever humans have access to additional information over the AI, there is potential to achieve *complementary performance* by pairing the two, i.e., better performance than either the human or AI alone. For example, a physician may have access to additional information that may not be captured in tabular electronic health records or other structured data [Alur et al., 2024].

Evidence of complementary performance between humans and AI nonetheless remains limited, with many studies showing that human-AI teams underperform an AI alone [Buçinca et al., 2020, Bussone et al., 2015, Green and Chen, 2019b, Jacobs et al., 2021, Lai and Tan, 2019, Vaccaro and Waldo, 2019, Kononenko, 2001]. A solid understanding of such results is limited by the fact that most analyses of human-AI decision-making focus on ranking the performance of human-AI teams or each individually using measures based on post hoc decision accuracy [Passi and Vorvoreanu, 2022]. This approach is problematic for several reasons. First, it does not account for the best achievable performance based on the information available at the time of the decision [Kleinberg et al., 2015, Guo et al., 2024, Rambachan, 2024]. Second, it cannot provide insight into the potential for available information to improve decision performance, making it difficult to design interventions that improve the team’s performance.

In contrast, identifying information complementarities that contribute to the maximum achievable decision performance of a human and AI model—such as when one of the agents has access to information not contained in the other’s judgments, or has not fully integrated information available in the environment into their judgments—provides actionable information for improving the decision pipeline. For example, the degree to which a model provides information that complements human judgments can guide AI model selection. Evidence that human experts possess decision-relevant information over AI predictions motivates further data collection to improve the AI model. Evidence

*Department of Computer Science, Northwestern University. Email: ziyang.guo@northwestern.edu

†Department of Computer Science, Northwestern University. Email: yifan.wu@u.northwestern.edu

‡Department of Computer Science, Northwestern University. Email: hartline@northwestern.edu

§Department of Computer Science, Northwestern University. Email: jhullman@northwestern.edu

that model predictions contain decision-relevant information that humans do not exploit can guide the design of explanations highlighting complementary information.

We contribute a decision-theoretic framework for characterizing the value of information available within an AI-assisted decision workflow. In our framework, information is considered valuable to a decision-maker to the extent that it is possible, in theory, to incorporate it into their decisions to improve performance. Specifically, our approach analyzes the expected marginal payoff gain from best case (Bayes rational) use of additional information over best case use of the information already encoded in agent decisions for a given decision problem. The intuition behind this approach is that any information that is used by the agents will eventually reveal itself through variation in their decisions. We identify the value of the information in agent (human, AI, or human-AI) decisions by offering them as a signal to a Bayesian rational decision-maker. While we focus on combinations of humans and AI agents, the methods we propose can be applied to any combination of agents.

We introduce two metrics for evaluating information value in human-AI collaboration. The first—global human-complementary information value—calculates the value of a new piece of information to an agent over all of its possible realizations among all instances. The second—instance-level human-complementary information value—identifies opportunities for decision-makers to better use instance-level information.

We demonstrate the framework by applying the metrics to three decision-making tasks where AI models serve as human decision-making assistants¹: chest X-ray diagnosis [Rajpurkar et al., 2018, Johnson et al., 2019], deepfake detection [Dolhansky et al., 2020, Groh et al., 2022], and recidivism prediction [Angwin et al., 2022, Dressel and Farid, 2018]. First, we demonstrate the framework’s utility in *model selection* by evaluating how well different AI models complement human decision-makers, showing how even among models with similar accuracy, some models strictly offer more *complementary* information than others across decision problems. Next, we use the framework to empirically evaluate how providing AI assistance (alongside instance-level features) helps humans exploit available information for decision-making. Lastly, we demonstrate use of the framework to design explanations by extending SHAP [Lundberg and Lee, 2017] to highlight the portion of an AI’s explanation that complements human information.

2 Related work

Human-AI complementarity. Many empirical studies of human-AI collaboration focus on AI-assisted human decision-making for legal, ethical, or safety reasons [Bo et al., 2021, Boskemper et al., 2022, Bondi et al., 2022, Schemmer et al., 2022]. However, a recent meta-analysis by Vaccaro et al. [2024] finds that, on average, human-AI teams perform worse than the better of the two agents alone. In response, a growing body of work seeks to evaluate and enhance complementarity in human-AI systems [Bansal et al., 2021b, 2019, 2021a, Wilder et al., 2021, Rastogi et al., 2023, Mozannar et al., 2024b]. The present work differs from much of this prior work by approaching human-AI complementarity from the perspective of information value and use, including asking whether the human and AI decisions provide additional information that is not used by the other.

Evaluation of human decision-making with machine learning. Our work contributes methods for evaluating the decisions of human-AI teams [Kleinberg et al., 2015, 2018, Lakkaraju et al., 2017, Mullainathan and Obermeyer, 2022, Rambachan, 2024, Guo et al., 2024, Ben-Michael et al., 2024, Shreeksumar, 2025]. Kleinberg et al. [2015] proposed that evaluations of human-AI collaboration should be based on the information that is available at the time of decisions. According to this view, our work defines Bayesian best-attainable-performance benchmarks similar to several prior works [Guo et al., 2024, Wu et al., 2023, Agrawal et al., 2020, Fudenberg et al., 2022]. Closest to our work, Guo et al. [2024] model the expected performance of a rational Bayesian agent faced with deciding between the human and AI recommendations as the theoretical upper bound on the expected performance of any human-AI team. This benchmark provides a basis for identifying exploitable information within a decision problem.

¹Code to replicate our experiments is available at https://osf.io/p2qzy/?view_only=ec06600d06cd4e59bb6051f992e54c08

Human information in machine learning. Some approaches focus on automating the decision pipeline by explicitly incorporating human expertise in developing machine learning models, such as by learning to defer [Mozannar et al., 2024a, Madras et al., 2018, Raghu et al., 2019, Keswani et al., 2022, 2021, Okati et al., 2021]. Corvelo Benz and Rodriguez [2023] propose multicalibration over human and AI model confidence information to guarantee the existence of an optimal monotonic decision rule. Alur et al. [2023] propose a hypothesis testing framework to evaluate the added value of human expertise over AI forecasts. Our work shares the motivation of incorporating human expertise, but targets a slightly broader scope by quantifying the information value for all available signals and agent decisions in a human–AI decision pipeline.

3 Methodology

Our framework takes as input a decision problem associated with an information model and outputs the value of information of any available signals to any agent, conditioning on the existing information in their decisions within a Bayesian decision theoretic framework. Our framework provides two separate functions to quantify the value of information: one globally across the data-generating process, and one locally in a realization drawn from the data-generating process. We also introduce a robust analysis approach to information order, which enables us to compare the agent-complementary information in signals for all possible decision problems.

Decision Problem. A decision problem consists of three key elements. We illustrate with an example of a weather decision.

- A payoff-relevant state ω from a space Ω . For example, $\omega \in \Omega = \{0, 1\} = \{\text{no rain}, \text{rain}\}$.
- A decision d from the decision space \mathbf{D} characterizing the decision-maker (DM)’s choice. For example, $d \in \mathbf{D} = \{0, 1\} = \{\text{not take umbrella}, \text{take umbrella}\}$.
- A payoff function $S : \mathbf{D} \times \Omega \rightarrow \mathbb{R}$, used to assess the quality of a decision given a realization of the state. For example, $S(d = 0, \omega = 0) = 0$, $S(d = 0, \omega = 1) = -100$, $S(d = 1, \omega = 0) = -50$, $S(d = 1, \omega = 1) = 0$, which punishes the DM for selecting an action that does not match the weather.

In decision problems corresponding to prediction tasks, the decision space is a probabilistic belief over the state space, i.e., $\mathbf{D} = \Delta(\Omega)$. For such problems, a payoff function is said to be a *proper* scoring rule if the optimal action is to predict the true distribution, i.e., $p = \arg \max_{d \in \mathbf{D}} \mathbf{E}_{\omega \sim p}[S(d, \omega)]$. For any decision problem with payoff function $S : \mathbf{D} \times \Omega \rightarrow \mathbb{R}$, there is an equivalent proper scoring rule $\hat{S} : \Delta(\Omega) \times \Omega \rightarrow \mathbb{R}$ defined by choosing the optimal decision under the reported belief. Formally,

$$\hat{S}(p, \omega) = S(\arg \max_{d \in \mathbf{D}} \mathbf{E}_{\omega \sim p}[S(d, \omega)], \omega). \quad (1)$$

Equation (1) shows a reduction from the payoff function S to the proper scoring rule \hat{S} , i.e., any decision p under \hat{S} represents a decision d in S that best-responds to the distribution p . Therefore, the best-attainable performance defined in the proper scoring rule \hat{S} is equivalent to the best-attainable performance defined in any payoff function S that can be reduced to \hat{S} . Throughout our framework, we prefer proper scoring rules over non-proper scoring rules, since the best-attainable performance defined in the former implies the best-attainable performance in the latter.

Information Model. We cast the information available to a DM as a signal defined within an information model. We use the definition of an information model in Blackwell et al. [1951]. The information model can be represented by a *data-generating model* with a set of *signals*.

- *Signals.* There are n “basic signals” represented as random variables $\Sigma_1, \dots, \Sigma_n$, from the signal spaces $\Sigma_1, \dots, \Sigma_n$. Basic signals represent information available to a decision-maker, e.g., $\Sigma_1 = \{\text{cloudy}, \text{not cloudy}\}$, $\Sigma_2 \in \{0, \dots, 100\}$ for temperature in Celsius, etc. The decision-maker observes a signal, which is a subset of the basic signals, $V \subseteq 2^{\{\Sigma_1, \dots, \Sigma_n\}}$. Specifically, we use $V = \{\Sigma_{j_1}, \dots, \Sigma_{j_k}\}$ for a signal having k basic signals and denote the signal space as $\mathbf{V} = \Sigma_{j_1} \times \dots \times \Sigma_{j_k}$. For example, a signal representing a combination of two basic signals $V = \{\Sigma_1, \Sigma_2\}$ observed by the decision-maker

might consist of cloudiness Σ_1 and the temperature Σ_2 of the day. Given a signal composed of m basic signals, we write the realization of V as $v = (\sigma_{j_1}, \dots, \sigma_{j_k})$, where the realizations $\sigma_{j_i} \in \Sigma_{j_i}$ are sorted by the index of the basic signals $j_i \in [n]$. The union V of two signals V_1, V_2 takes the set union, i.e., $V = V_1 \cup V_2$.

- *Data-generating process.* A data-generating process is a joint distribution $\pi \in \Delta(\Sigma_1 \times \dots \times \Sigma_n \times \Omega)$ over the basic signals and the payoff-relevant state. π can be viewed as the combination of two distributions: the prior distribution of the state $\Pr[\omega]$ and the signal-generating distribution $\Pr[v|\omega]$ defining the conditional distribution of signals. The DM may only observe a subset V of the n basic signals. We can define the Bayesian posterior belief upon receiving a signal $V = v$ from the data-generating model as

$$\pi(\omega|v) := \Pr[\omega|v] = \frac{\pi(v, \omega)}{\pi(\omega)}$$

where we slightly abuse notation to write $\pi(v, \omega)$ as the marginal probability of the signal realized to be v and the state being ω with expectation over other signals.

The choice of basic signals directly impacts how many observed samples are required to get a good estimate of the data-generating process. When high-dimensional signals such as images or text are used, it may not be computationally feasible to estimate the data-generating process. In such cases, one can preprocess the high-dimensional signals to get low-dimensional representations which (ideally) capture any important structure. These lower-dimensional signals can be defined by humans, such as when concepts are identified and then used to label the high-dimensional signals (e.g., images or parts of images). Alternatively, they can be defined algorithmically, by strategically applying dimensionality reduction to generate low-dimensional embeddings. We introduce an algorithm for identifying an “optimal” reduction model in decision problems in Appendix B. We demonstrate these two methods in Section 4 and Section 5 respectively.

Information value. Our framework quantifies the value of information in a signal V as the expected payoff improvement of an idealized agent who has access to V in addition to some baseline information set. We suppose a rational Bayesian DM who knows the prior probability of the state and conditional distribution of signals (i.e., the data-generating process), observes a signal realization, updates their prior to arrive at posterior beliefs, and then chooses a decision to maximize their expected payoff given their posterior belief. Formally, given a decision task with payoff function S and an information model π , the rational DM’s expected payoff given a (set of) signal(s) V is

$$R^{\pi, S}(V) = \mathbf{E}_{(v, \omega) \sim \pi}[S(d^r(v), \omega)] \quad (2)$$

where $d^r(\cdot) : \mathbf{V} \rightarrow \mathbf{D}$ denotes the decision rule adopted by the rational DM.

$$d^r(v) = \arg \max_{d \in \mathbf{D}} \mathbf{E}_{\omega \sim \pi(\omega|v)}[S(d, \omega)] \quad (3)$$

We use \emptyset to represent a null signal, such that $R^{\pi, S}(\emptyset)$ is the expected payoff of a Bayesian rational DM who only uses the prior distribution to make decisions. In this case, the Bayesian rational DM will take the best fixed action under the prior, and their expected payoff is:

$$R^{\pi, S}(\emptyset) = \max_{d \in \mathbf{D}} \mathbf{E}_{\omega \sim \pi}[S(d, \omega)] \quad (4)$$

This baseline defines the maximum expected payoff that can be achieved with no information. Bayesian decision theory quantifies the information value of V by the payoff improvement of V over the payoff obtained without information.

Definition 3.1. Given a decision task with payoff function S and an information model π , the information value of V is defined as

$$IV^{\pi, S}(V) = R^{\pi, S}(V) - R^{\pi, S}(\emptyset) \quad (5)$$

We adopt the same idea to define the agent-complementary information value in our framework.

3.1 Agent-Complementary Information Value

With the above definitions, it is possible to measure the additional value that new signals can provide over the information already captured by an agent’s decisions. Here, *agent* may refer to a human, an AI system, or a human–AI team. The intuition behind our approach is that any information that is used by decision-makers should eventually reveal itself through variation in their decisions. We recover the information value in agent decisions by offering the decisions as a signal to the Bayesian rational DM. We model the agent decisions as a random variable D^b from the action space \mathbf{D} , which follows a joint distribution $\pi \in \Delta(\Sigma_1 \times \dots \times \Sigma_n \times \Omega \times \mathbf{D})$ with the state and signals. The expected payoff of a Bayesian rational DM who knows π is given by the function:

$$R^{\pi,S}(D^b) = \mathbf{E}_{(d^b, \omega) \sim \pi}[S(d^r(d^b), \omega)]$$

We seek to identify signals V that can potentially improve agent decisions by analyzing the information value in the combined signal $D^b \cup V$ over the information value in D^b , which we define as the agent-complementary information value.

Definition 3.2. Given a decision task with payoff function S and an information model π , we define the agent-complementary information value (ACIV) of V on agent decisions D^b as

$$\text{ACIV}^{\pi,S}(V; D^b) = R^{\pi,S}(D^b \cup V) - R^{\pi,S}(D^b) \quad (6)$$

If the ACIV of a signal V is small relative to the baseline (4), this means either that the information value of V to the decision problem is low (e.g., it is not correlated with ω), or that the agent has already exploited the information in V (e.g., the agent relies on V or equivalent information to make their decisions such that their decisions correlate with ω in the same way as V correlates with ω). If, however, the ACIV of V is large relative to the baseline, then at least in theory, the agent can improve their payoff by incorporating V in their decision making.

Furthermore, ACIV can reveal complementary information between different types of agents. For instance, if we view AI predictions as V and treat human decisions as the agent signal D^b , a large ACIV indicates that AI predictions add considerable value beyond what humans alone achieve. In the reverse scenario, if human decisions serve as V and AI predictions are D^b , we can measure how much humans can contribute over the information captured in the AI predictions. We demonstrate uses of ACIV in Section 4 and Section 5.

3.2 Instance-level Agent-complementary Information Value

ACIV quantifies the value of the decision-relevant information in a signal V across all possible realizations defined by the data-generating model. To provide analogous instance-level quantification of information value, we define Instance-Level agent-complementary Information Value (ILIV) to quantify the value of the decision-relevant information encoded by a single realization of the signal. This finer-grained view makes it possible to analyze how much an agent can benefit in theory from better incorporating instance-level information in their decision.

Given a realization of signal $v = \{\sigma_{j_1}, \dots, \sigma_{j_k}\}$, we want to know the maximum expected payoff gain from gaining access to v on the instances where v is realized over the existing information encoded in agent decisions. Intuitively, this captures how much “room” there is for specific decisions to be improved through better use of the signal. To calculate instance-level information value, we rely on the performance of the Bayesian rational agent on the conditional distribution $\pi(\sigma_1, \dots, \sigma_n, \omega, d^b | v)$ instead of the whole distribution $\pi(\sigma_1, \dots, \sigma_n, \omega, d^b)$. Formally, given a decision task with payoff function S and information model π , the expected payoff of the rational DM given signal $V = v$ on instances where $V = v$ is

$$r^{v,\pi,S}(v) = \mathbf{E}_{\omega \sim \pi(\omega | v)}[S(d^r(v), \omega)] \quad (7)$$

where $d^r(v)$ is the Bayesian optimal decision on receiving v as defined in Equation (3). If we consider the agent decisions in addition to the realization v , the rational DM’s expected payoff on instances where $V = v$ can be written as

$$r^{v,\pi,S}(v; D^b) = \mathbf{E}_{(d^b, \omega) \sim \pi(d^b, \omega | v)}[S(d^r(v \cup d^b), \omega)] \quad (8)$$

Definition 3.3. Given a decision task with payoff function S and an information model π , we define the instance-level agent-complementary information value (ILIV) of signal $V = v$ on instances where $V = v$ as:

$$\text{ILIV}^{v,\pi,S}(v; D^b) = \mathbf{r}^{v,\pi,S}(v; D^b) - \mathbf{r}^{v,\pi,S}(\emptyset; D^b) \quad (9)$$

where $\mathbf{r}^{v,\pi,S}(\emptyset; D^b)$ represents the rational DM’s expected payoff on instances where $V = v$ with only the existing information encoded in agent decisions. Taking the expectation of ILIV over V recovers the global agent-complementary information value (ACIV), i.e.,

$$\text{ACIV}^{\pi,S}(V; D^b) = \mathbf{E}_{v \sim \pi(v)}[\text{ILIV}^{v,\pi,S}(v; D^b)]$$

3.2.1 ILIV-SHAP Information-based Explanation

We apply ILIV to define an *information-based* explanation technique (ILIV-SHAP) that extends the canonical SHAP feature saliency explanation of a model’s prediction. ILIV-SHAP communicates how the data features lead to changes in the information value of AI predictions. While traditional SHAP summarizes the average contribution of each feature to a specific prediction over the baseline (prior) prediction, ILIV-SHAP summarizes the average contribution of each feature to the decision-relevant information value contained in the prediction.

Suppose a model f that takes as input m features and outputs a real number. Given an instance $\mathbf{x} = (x_1, \dots, x_m)$, the importance of one feature x_i to the model output $f(\mathbf{x})$ is encoded by the expected difference of model outputs when x_i is marginalized out. Specifically, this is quantified by $f(\mathbf{x}) - \mathbf{E}[f(X)|X_{-i} = \mathbf{x}_{-i}]$, where X_{-i} denotes all features except X_i . Considering the interaction between features, SHAP [Lundberg and Lee, 2017] uses the Shapley value to quantify the importance scores averaged on different combinations of features:

$$\phi_i(f, \mathbf{x}) = \sum_{\mathbf{x}' \subseteq \mathbf{x}} \frac{|\mathbf{x}'|!(m - |\mathbf{x}'| - 1)!}{m!} [g_f(\mathbf{x}') - g_f(\mathbf{x}' \setminus x_i)]$$

where $g_f(\mathbf{x}')$ denotes the expected model output conditioned on \mathbf{x}' , i.e., $\mathbf{E}[f(X)|X' = \mathbf{x}']$ for any $\mathbf{x}' \subseteq \mathbf{x}$. The scores $\phi_i(f, \mathbf{x})$ output by SHAP construct an explanation model for a model output, which quantifies the expected counterfactual change in the model output caused by the feature x_i .

ILIV-SHAP extends SHAP to give an explanation model on how features impact the decision-relevant information value of an individual model output.

Definition 3.4 (ILIV-SHAP). Given a model f and data features $\mathbf{x} = (x_1, \dots, x_m)$, the importance score of the i -th feature by ILIV-SHAP is

$$\phi_i^{\text{ILIV}}(f, \mathbf{x}) = \sum_{\mathbf{x}' \subseteq \mathbf{x}} \frac{|\mathbf{x}'|!(m - |\mathbf{x}'| - 1)!}{m!} [\text{ILIV}^{f(\mathbf{x}),\pi,S}(g_f(\mathbf{x}'); D^b) - \text{ILIV}^{f(\mathbf{x}),\pi,S}(g_f(\mathbf{x}' \setminus x_i); D^b)]$$

where $\text{ILIV}^{f(\mathbf{x}),\pi,S}(g_f(\mathbf{x}'); D^b)$ denotes a counterfactual evaluation of ILIV, which quantifies the expected payoff gain from additionally knowing $g_f(\mathbf{x}')$ on the instances where $f(\mathbf{x})$ is realized. This counterfactual version of ILIV is guaranteed to achieve the maximum at \mathbf{x}' where $f(\mathbf{x}) = g_f(\mathbf{x}')$, i.e., the features missing from \mathbf{x}' have no impact on $f(\mathbf{x})$.

The explanation model offered by ILIV-SHAP is grounded in the following two properties. First, $\phi_i^{\text{ILIV}}(f, \mathbf{x})$ are consistent with the extent to which feature x_i contributes to the information value in $f(\mathbf{x})$. Specifically, for any two models f and f' and any $\mathbf{x}' \subseteq \mathbf{x}$, if x_i contributes more to the information value in f' than the information value in f , i.e., $\text{ILIV}^{f'(\mathbf{x}),\pi,S}(g_{f'}(\mathbf{x}'); D^b) - \text{ILIV}^{f'(\mathbf{x}),\pi,S}(g_{f'}(\mathbf{x}' \setminus x_i); D^b) \geq \text{ILIV}^{f(\mathbf{x}),\pi,S}(g_f(\mathbf{x}'); D^b) - \text{ILIV}^{f(\mathbf{x}),\pi,S}(g_f(\mathbf{x}' \setminus x_i); D^b)$, then $\phi_i^{\text{ILIV}}(f', \mathbf{x}) \geq \phi_i^{\text{ILIV}}(f, \mathbf{x})$. This property of ILIV-SHAP follows the consistency property of SHAP [Lundberg and Lee, 2017]. Second, summing up the scores $\phi_i^{\text{ILIV}}(f, \mathbf{x})$ recovers the information value of model output, $\text{ILIV}^{f(\mathbf{x}),\pi,S}(f(\mathbf{x}); D^b)$. Formally, for any f and any \mathbf{x} , $\text{ILIV}^{f(\mathbf{x}),\pi,S}(f(\mathbf{x}); D^b) = \text{ILIV}^{f(\mathbf{x}),\pi,S}(\mathbf{E}[f(X)]; D^b) + \sum_{i=1}^m \phi_i^{\text{ILIV}}(f, \mathbf{x})$. We demonstrate use of ILIV-SHAP in Section 6.

3.3 Robustness Analysis of Information Order

Our approach assumes the specification of a decision problem on which agents’ decisions and use of information are evaluated. However, ambiguity around the appropriate decision problem, and in particular, the appropriate scoring rule, is not uncommon in human-AI decision settings. Ambiguity can arise as a result of challenges in eliciting utility functions and/or variance in these functions across decision-makers or groups of instances; for example, doctors penalize certain false negative results differently when diagnosing younger versus older patients [McLaughlin and Spiess, 2023]. Blackwell’s comparison of signals [Blackwell et al., 1951] is an appropriate tool for addressing ambiguity about the payoff function, as it defines a (set of) signal V_1 as *more informative* than V_2 if V_1 has a higher information value on all possible decision problems. We identify this partial order by decomposing the space of decision problems via a basis of proper scoring rules² [Li et al., 2022, Kleinberg et al., 2023].

Definition 3.5 (Blackwell Order of Information). A signal V_1 is Blackwell more informative than V_2 if V_1 achieves a higher best-attainable payoff on any decision problems:

$$R^{\pi, S}(V_1) \geq R^{\pi, S}(V_2), \forall S$$

The Blackwell order is evaluated over all possible decision problems, which cannot be tested directly. Fortunately, we only need to test over all proper scoring rules since any decision problem can be represented by an equivalent proper scoring rule, and the space of proper scoring rules can be characterized by a set of V-shaped scoring rules. A V-shaped scoring rule is parameterized by the kink of the piecewise-linear utility function.

Definition 3.6. (V-shaped scoring rule) A V-shaped scoring rule with kink $\mu \in (0, \frac{1}{2}]$ is defined as

$$S_\mu(d, \omega) = \begin{cases} \frac{1}{2} - \frac{1}{2} \cdot \frac{\omega - \mu}{1 - \mu} & \text{if } d \leq \mu \\ \frac{1}{2} + \frac{1}{2} \cdot \frac{\omega - \mu}{1 - \mu} & \text{else,} \end{cases}$$

When $\mu' \in (\frac{1}{2}, 1)$, the V-shaped scoring rule can be symmetrically defined by $S_{\mu'} = S_{1-\mu'}(1-y, \omega)$.

Intuitively, the kink μ represents the threshold belief where the decision-maker switches between two actions. Larger μ means that the decision-makers will prefer $d = 1$ more. The closer μ is to 0.5, the more indifferent the decision-maker is to $d = 0$ or $d = 1$.

Proposition 3.7 shows that if V_1 achieves a higher information value on the basis of V-shaped proper scoring rules than V_2 , then V_1 is Blackwell more informative than V_2 . Proposition 3.7 follows from the fact that any best-responding payoff can be linearly decomposed into the payoff on V-shaped scoring rules.

Proposition 3.7 (Hu and Wu 2024). If $\forall \mu \in (0, 1)$

$$R^{\pi, S_\mu}(V_1) \geq R^{\pi, S_\mu}(V_2),$$

then V_1 is Blackwell more informative than V_2 .

Extending this to agent-complementary information value, we say that V_1 offers a higher complementary value than V_2 under the Blackwell order if

$$\text{ACIV}^{\pi, S_\mu}(V_1; D^b) \geq \text{ACIV}^{\pi, S_\mu}(V_2; D^b), \forall \mu \in (0, 1)$$

This definition allows us to rank signals (or sets of signals) without needing to commit to a specific payoff function. We present a use case in Section 4.

4 Experiment I: Model Comparison on Chest Radiograph Diagnosis

We apply our framework to a well-known cardiac dysfunction diagnosis task [Rajpurkar et al., 2018, Tang et al., 2020, Shree Kumar, 2025]. We demonstrate how our framework can be used in model evaluation for analyzing how much complementary information value a set of possible AI models offers to the radiology reports written by experts.

²For rational DMs, any decision problem can be represented by an equivalent proper scoring rule in Equation (1), such that the partial order defined via proper scoring rules also applies to the corresponding decision tasks.

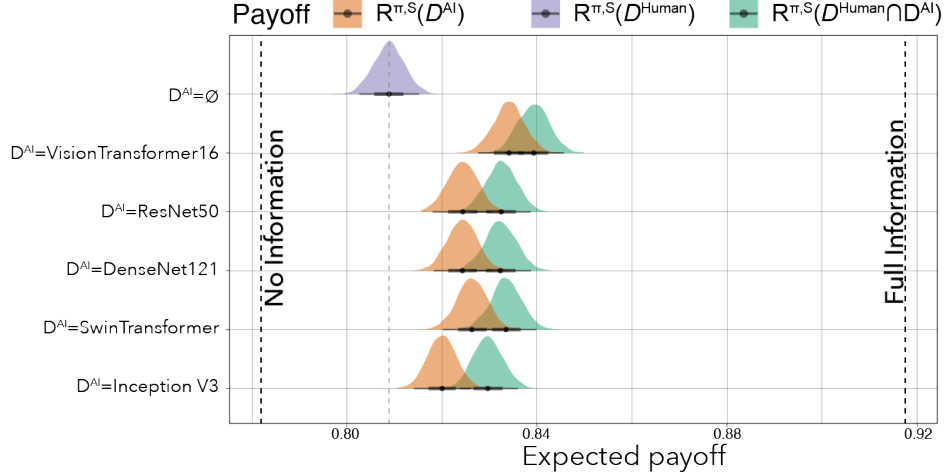


Figure 1: Information value of all deep-learning models calculated under our framework. The first row represents the human-alone decisions (without considering any AI predictions as additional signals). The other rows are the combinations of the human-alone decisions and the AI predictions from different pre-trained models. We list the AI predictions alone to show the AI-complementary information value offered by human decisions.

4.1 Data and Model

We use data from the MIMIC dataset [Goldberger et al., 2000], which contains anonymized electronic health records from Beth Israel Deaconess Medical Center (BIDMC), a large teaching hospital in Boston, Massachusetts, affiliated with Harvard Medical School. Specifically, we utilize chest x-ray images and radiology reports from the MIMIC-CXR database [Johnson et al., 2019] merged with patient and visit information from the broader MIMIC-IV database [Johnson et al., 2023]. The payoff-related state, cardiac dysfunction $\omega \in \{0, 1\}$, is coded based on two common tests, the NT-proBNP and the troponin, using the age-specific cutoffs from Mueller et al. [2019] and Heidenreich et al. [2022]. We label the radiology reports by a rule-based tool [Irvin et al., 2019] and use the labels as the human decisions (without AI assistance) in the diagnosis task to solve the problem of computational feasibility with high-dimensional textual reports. The labels are represented by the symptoms as positive, negative, or uncertain, i.e., $d \in \{+, ?, -\}$. We fine-tuned five deep-learning models on the cardiac dysfunction diagnosis task, VisionTransformer [Alexey, 2020], SwinTransformer [Liu et al., 2021], ResNet [He et al., 2016], Inception-v3 [Szegedy et al., 2016], and DenseNet [Huang et al., 2017]. Our training set contains 12,228 images, and the validation set contains 6,115 images. On a hold-out test set with 12,229 images, the AUC achieved by the five models is: DenseNet with 0.77, Inception v3 with 0.76, ResNet with 0.77, SwinTransformer with 0.78, and VisionTransformer with 0.80.

We consider Brier score, a.k.a., quadratic score, as the payoff function: $S(\omega, d) = 1 - (\omega - d)^2$. The scale of the quadratic score is $[0, 1]$ and a random guess ($d \sim \text{Bernoulli}(0.5)$) achieves 0.75 payoff. We use the quadratic score instead of the mean absolute error that is usually used in cardiac dysfunction diagnosis task because the quadratic score is a proper scoring rule where truthfully reporting the belief maximizes the payoff³. We also conduct a robust analysis considering various V-shaped payoff functions with different kinks on a discretized grid of $[0, 1]$ with a step of 0.01. We use the hold-out test set to estimate the data-generating process, which defines the joint distribution of state, human decisions, and AI models' predictions.

We construct the scale of performances by a no-information bound and a full-information bound. The no-information bound is $R^{\pi, S}(\emptyset)$, the baseline as we define the information value. The full-information bound is defined as the expected payoff of a rational DM who has access to all signals, human label from radiology report and predictions from five AI models. We do not consider the radiology images as a basic signal in this task because of the problem of computational feasibility with high-dimensional signals. We use the five vision models' predictions as embeddings of the original

³We prefer a proper scoring rule so that the rational decision-maker's strategy is to reveal their true belief, ensuring that the signal's information value accurately reflects its role in forming beliefs.

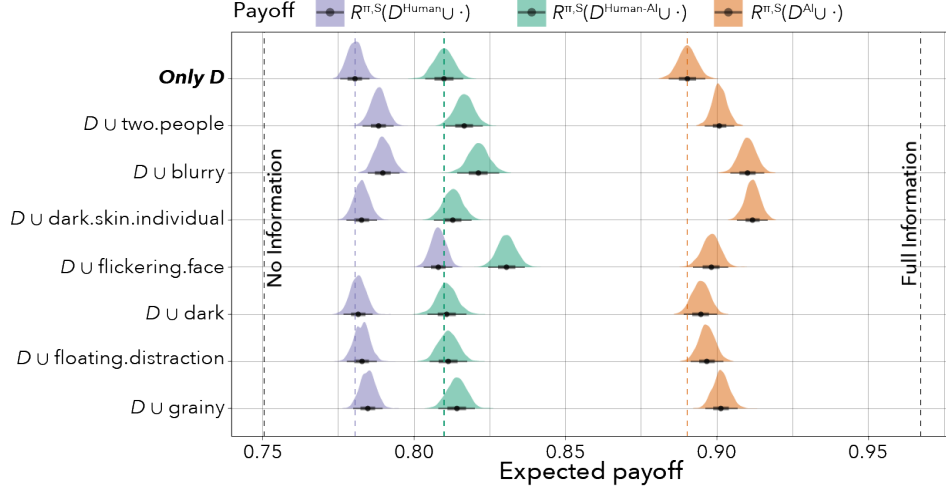


Figure 2: Information value calculated under our framework in the information model defined by the experiment of Groh et al. [2022]. Basic signals include the seven video level features and three types of agent decisions. The baseline on the left represents the expected payoff given no information, i.e., $R^{\pi,S}(\emptyset)$, and the benchmark on the right represents the expected payoff given all available information, i.e., $R^{\pi,S}(\{\Sigma_1, \dots, \Sigma_n, D^{\text{Human}}, D^{\text{Human-AI}}, D^{\text{AI}}\})$. All the payoffs are calculated by $R^{\pi,S}(\cdot)$, where \cdot is the signal on the y -axis.

images. See more detail on the algorithm of choosing the optimal embeddings in Appendix B.

4.2 Results

Can the AI models complement human judgment? We first analyze the agent-complementary information values in Figure 1, using the Brier score as the payoff function. We find that all AI models provide complementary information value to the aforementioned human judgment. As shown in Figure 1 (comparison between $R^{\pi,S}(D^{\text{Human}} \cup D^{\text{AI}})$ and $R^{\pi,S}(D^{\text{Human}})$), all AI models capture at least 20% of the total available information value (across all AI model and human decisions) that is not exploited by human decisions. This motivates deploying an AI to assist humans in this scenario.

In the other direction, the human decisions also provide complementary information to all AI models, comparing $R^{\pi,S}(D^{\text{Human}})$ with $R^{\pi,S}(D^{\text{AI}})$ in Figure 1. This observation might inspire, for example, further investigation of the information the humans can access to that is not represented in AI training data.

Which AI model offers the most decision-relevant information over human judgments?

Figure 1 shows that VisionTransformer contains slightly higher information value than the other models, and Inception v3 contains slightly lower information value than the other models. We assess the stability of VisionTransformer’s superiority over the other AI models across many possible losses to test if there is a Blackwell ordering of models. By Proposition 3.7, we test the payoff of models on all V-shaped scoring rules, shown in Figure 4. Across all the V-shaped payoff functions, we find that VisionTransformer is Blackwell more informative and Inception v3 is Blackwell less informative than all other models. The VisionTransformer achieves a higher information value on all V-shaped scoring rules, implying a higher information value on all decision problems.

5 Experiment II: Behavioral Analysis on Deepfake Detection

We apply our framework to analyze a deepfake video detection task [Dolhansky et al., 2020], where participants are asked to judge whether a video was created by generative AI, including with the assistance of an AI model.

5.1 Data and Model

We define the information model on the experiment data of Groh et al. [2022]. Non-expert participants ($n=5,524$) were recruited through Prolific and asked to examine the videos. They reported their decisions in two rounds. They first reviewed the video and reported an *initial* decision (D^{Human}) without access to the AI model. Then, in a second round, they were provided with the recommendation (D^{AI}) of a multitask cascaded convolutional neural network [Zhang et al., 2016], with estimated 65% accuracy on holdout data, and chose whether to change their initial decision. This produced a *final* decision ($D^{\text{Human-AI}}$). Both decisions were elicited as a percentage indicating how confident the participant was that the video was a deepfake, measured in 1% increments: $d \in \{0\%, 1\%, \dots, 100\%\}$. We round the predictions from the AI model to the same 100-scale probability scale available to study participants.

We use the Brier score as the payoff function, with the binary payoff-related state: $\omega \in \{0, 1\} = \{\text{genuine}, \text{fake}\}$. This choice differs from the mean absolute error used by Groh et al. [2022], but again we use the quadratic score because it is a proper scoring rule where truthfully reporting the belief maximizes the score.

We identify a set of features that were implicitly available to all three agents (human, AI, and human-AI). Because the video signal is high dimensional, we make use of seven video-level features using manually coded labels by Groh et al. [2022]: graininess, blurriness, darkness, presence of a flickering face, presence of two people, presence of a floating distraction, and the presence of an individual with dark skin, all of which are labeled as binary indicators. These are the basic signals in our framework. We estimate the data-generating process π using the realizations of signals, state, first-round human decisions, AI predictions, and second-round human-AI decisions. The no-information bound is the same as Section 4 while the full-information bound is defined as the expected payoff of a rational DM who has access to all video-level features and three agents’ decisions.

5.2 Results

How much decision-relevant information do agents’ decisions offer? We first compare the information value of the AI predictions to that of the human decisions in the first round (without AI assistance). Figure 2(a) shows that **AI predictions** provide about 65% of the total possible information value over the no-information baseline, while **human decisions** only provide about 15%. Because the no information baseline, 0.75, is equivalent to a random guess drawn from Bernoulli(0.5), human decisions are only weakly informative for the problem.

We next consider the **human-AI decisions**. Given that the AI predictions contain a significant portion of the total possible information value, we might hope that when participants have access to the AI predictions, their performance will be close to the full information baseline. However, the information value of the **human-AI decisions** only achieves a small proportion of the total possible information value (30%). This is consistent with the findings of Guo et al. [2024] that humans are bad at distinguishing when AI predictions are correct.

How much additional decision-relevant information do the available features offer over agents’ decisions? To understand what information might improve human decisions, we assess the ACIVs of different signals over different agents. This describes the additional information value in the signal after conditioning on the existing information in the agents’ decisions. As shown on the fifth row in Figure 2, the presence of a flickering face offers larger ACIV over human decisions than over AI predictions, meaning that human decisions could improve by a greater amount if they were to incorporate this information. Meanwhile, as shown on the fourth row in Figure 2, the presence of an individual with dark skin offers larger ACIV over AI predictions than over human decisions, suggesting that humans make greater use of this information. This suggests that the AI and human rely on differing information to make their initial predictions, where the AI relies more on information associated with the presence of a flickering face while human participants rely more on information associated with the presence of an individual with dark skin.

By comparing the ACIVs of different signals over human decisions and human-AI decisions, we also find that simply displaying AI predictions to humans did not lead to the AI-assisted humans exploiting the observed signals in their decisions. As shown in Figure 2, with the assistance of AI, the ACIVs of all signals over the human-AI teams’ decisions do not change much compared to the ACIVs over human decisions, with the exception of a slight improvement in the presence of a flickering face.

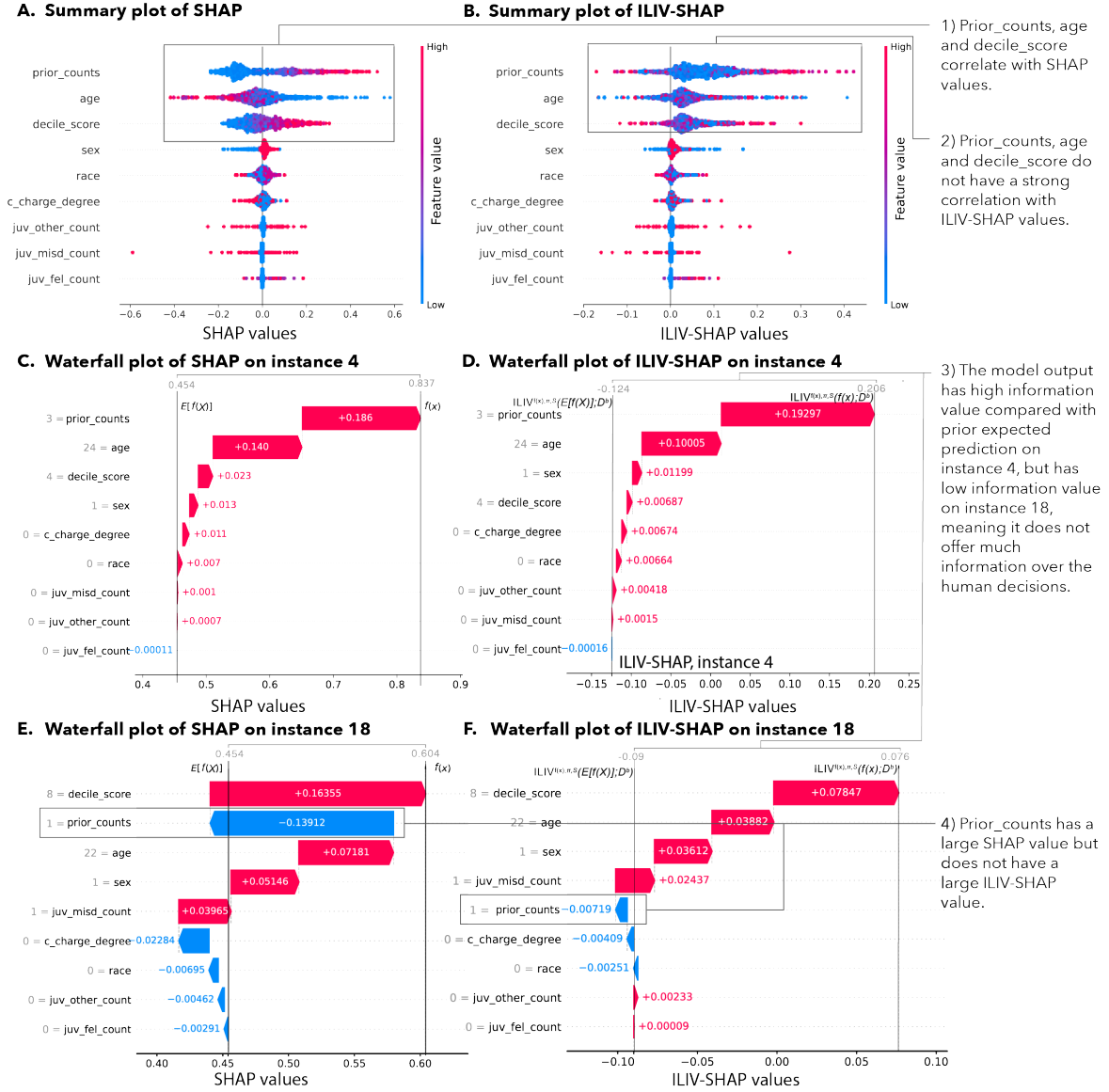


Figure 3: (A) Summary of SHAP explanation and (B) summary of ILIV-SHAP explanation, where each point represents an instance from the test set. (C-F) Waterfall plots of applying SHAP and ILIV-SHAP on instance 4 and instance 18. The Waterfall plot starts from the prior expected prediction (or ILIV of the prior expected prediction), and then adds features one at a time until reaching the current model output (or ILIV of the current model output). See further comparisons between SHAP and ILIV-SHAP in Appendix D.

This finding further confirms the hypothesis that humans are simply relying on AI predictions without processing the information contained in them.

6 Experiment III: Information-based Local Explanation on Recidivism Prediction

We apply our framework to a recidivism prediction task, where the decision-maker decides whether to release a defendant. We demonstrate using the framework to augment SHAP.

6.1 Data and Model

We use the COMPAS dataset [Angwin et al., 2022], which contains 11,758 defendants with associated features capturing demographics, information about their current charges, and their prior criminal history. We merge the dataset with the experimental data from Lin et al. [2020] to obtain human decisions, in the form of recidivism decisions on a subset of instances from Angwin et al. [2022]’s experiment on laypeople. Human decisions were elicited on a 30-point probability scale. Merging the two datasets produces 9,269 instances (defendants). For the AI model, we trained an extreme gradient boosting (XGBoost) model [Chen and Guestrin, 2016] on a training set with 6,488 instances, achieving an AUC of 0.84 on a hold-out test set with 2,781 instances. We round the model predictions to the same 30-point probability scale available to study participants in Lin et al. [2020].

We use the Brier score as the payoff function, which is commonly used in previous studies on recidivism [Green and Chen, 2019a, Lin et al., 2020, Fogliato et al., 2021]. The binary payoff-related state ω indicates whether the defendant gets rearrested within two years. We use the features of the defendant contained in the COMPAS dataset as the signals in our demonstration: demographic features (age, sex, and race), information about the current charge (type of offense and whether it is a misdemeanor or a felony), prior criminal history (e.g., past number of arrests and charges for several offense categories), and the predicted score from the COMPAS system⁴. We take the empirical distribution of the hold-out test set as the data-generating process, which defines the joint distribution of state, signals, human decisions, and AI predictions.

6.2 Results

SHAP explanations do not communicate the complementary information of AI predictions. Specifically, the changes in information value of AI predictions caused by marginalizing out features, i.e., ILIV-SHAP scores, are not predictable from the changes in AI predictions, i.e., SHAP scores, and the feature values. Figure 3 (A) and (B) compare the distribution of feature importance scores from SHAP to those from ILIV-SHAP. The scores of `prior_counts` (the number of prior criminal charges), `age`, and `decile_score` (the score from the COMPAS system), which are three features with the largest scores in both SHAP and ILIV-SHAP, show different correlations with the feature values in SHAP and ILIV-SHAP. For instance, in Figure 3(A), most of the low values (blue dots) of `prior_counts` have a negative SHAP score, and most of the high values (red dots) have a positive SHAP score. This indicates that when the value of `prior_counts` is low, marginalizing out `prior_counts` from the features leads to a higher expected model prediction than not marginalizing out, and vice versa. However, this correlation does not hold for ILIV-SHAP. In Figure 3(B), the high values of `prior_counts` appear on both the left side (below zero) and the right side (above zero), indicating having low ILIV-SHAP scores and high ILIV-SHAP scores at the same time. This mismatch between the distributions of SHAP scores and ILIV-SHAP scores implies that the impact of features on the information value cannot be directly inferred (at least monotonically) from their impact on model output and their values.

ILIV-SHAP can augment SHAP on communicating the complementary information of AI predictions. We argue that ILIV-SHAP can supplement saliency-based explanations to provide users with a sense of how the AI predictions can help improve their decisions. With ILIV-SHAP, users can check whether the prediction contains decision-relevant information by looking at the total ILIV of the AI prediction, which indicates the maximum improvement in expected payoff that could be achieved by incorporating this prediction. Figure 3(D) and (F) show two different cases, where the AI predictions contain substantial human-complementary information value in (D) (shown by the distance between the tail and the head of the Waterfall plot) but very little information in (F).

ILIV-SHAP also tells the user whether an AI model’s prediction encodes useful complementary information from a particular feature. In Figure 3(E), the defendant’s prior count record (`prior_counts=1`) ranks second among features that impact the AI prediction (-0.139). Upon seeing this, users might be interested in investigating how the AI uses `prior_counts=1`. However, Figure 3(F) shows that `prior_counts=1` contributes marginally to the decision-relevant information in AI predictions (about $+0.007$). Thus, with ILIV-SHAP, users can see that even if `prior_counts=1` changes the AI prediction significantly, the AI does not predict more accurately as a result of it.

⁴<https://doc.wi.gov/Pages/AboutDOC/COMPAS.aspx>

7 Discussion and Limitations

We propose a decision-theoretic framework for assigning value to information in human-AI decision-making. Our methods quantify the additional information value of any signals over an agent’s decisions, and can be applied to any combination of artificial or human agent judgments. The three demonstrations we provide show how quantified information value can drive model selection, empirical evaluation, and explanation design. These are just a few of many possible use cases. For example, explanation approaches could be compared in terms of their information value to human decisions. Information value analysis could also drive elicitation of human private signals upon identifying that human decisions contain AI-complementary information. New explanation strategies based on ILIV-SHAP could more directly integrate visualized information value with conventional depictions of feature importance.

It is important to note that when using ACIV to understand complementary information over human decisions, it cannot be interpreted as definitively establishing that particular signals were *used* by the human. It is always possible that the human has other private signals offering equivalent information to a feature being analyzed. This raises a question of whether it is definitive about use if it is an AI as the agent instead of a human. However, quantifying the value of observed information is an important first step toward learning about information that may exist beyond an explicit problem definition.

Our framework quantifies the best-attainable performance improvement from integrating signals in decisions. This does not necessarily mean that highlighting or otherwise emphasizing those signals for humans will lead to them performing better. However, the basis of our framework in Bayesian decision theory means that it provides a theoretical basis that can be adapted to support comparisons to human behavior to drive learning [Hullman and Gelman, 2021]. For example, if we suspect a human decision-maker uses AI predictions and their own predictions strictly monotonically, we could constrain the rational decision-maker to only make monotonic decisions with AI prediction and their own predictions.

References

- Stefanía Ægisdóttir, Michael J White, Paul M Spengler, Alan S Maugherman, Linda A Anderson, Robert S Cook, Cassandra N Nichols, Georgios K Lampropoulos, Blain S Walker, Genna Cohen, et al. The meta-analysis of clinical judgment project: Fifty-six years of accumulated research on clinical versus statistical prediction. *The Counseling Psychologist*, 34(3):341–382, 2006.
- Mayank Agrawal, Joshua C Peterson, and Thomas L Griffiths. Scaling up psychology via scientific regret minimization. *Proceedings of the National Academy of Sciences*, 117(16):8825–8835, 2020.
- Dosovitskiy Alexey. An image is worth 16x16 words: Transformers for image recognition at scale. *arXiv preprint arXiv: 2010.11929*, 2020.
- Rohan Alur, Loren Laine, Darrick Li, Manish Raghavan, Devavrat Shah, and Dennis Shung. Auditing for human expertise. *Advances in Neural Information Processing Systems*, 36:79439–79468, 2023.
- Rohan Alur, Manish Raghavan, and Devavrat Shah. Distinguishing the indistinguishable: Human expertise in algorithmic prediction. *arXiv preprint arXiv:2402.00793*, 2024.
- Julia Angwin, Jeff Larson, Surya Mattu, and Lauren Kirchner. Machine bias. In *Ethics of data and analytics*, pages 254–264. Auerbach Publications, 2022.
- Gagan Bansal, Besmira Nushi, Ece Kamar, Daniel S Weld, Walter S Lasecki, and Eric Horvitz. Updates in human-ai teams: Understanding and addressing the performance/compatibility tradeoff. In *Proceedings of the AAAI Conference on Artificial Intelligence*, volume 33, pages 2429–2437, 2019.
- Gagan Bansal, Besmira Nushi, Ece Kamar, Eric Horvitz, and Daniel S Weld. Is the most accurate ai the best teammate? optimizing ai for teamwork. In *Proceedings of the AAAI Conference on Artificial Intelligence*, volume 35, pages 11405–11414, 2021a.
- Gagan Bansal, Tongshuang Wu, Joyce Zhou, Raymond Fok, Besmira Nushi, Ece Kamar, Marco Tulio Ribeiro, and Daniel Weld. Does the whole exceed its parts? the effect of ai explanations on complementary team performance. In *Proceedings of the 2021 CHI Conference on Human Factors in*

- Computing Systems*, CHI '21, New York, NY, USA, 2021b. Association for Computing Machinery. ISBN 9781450380966. doi: 10.1145/3411764.3445717. URL <https://doi.org/10.1145/3411764.3445717>.
- Eli Ben-Michael, D James Greiner, Melody Huang, Kosuke Imai, Zhichao Jiang, and Sooahn Shin. Does ai help humans make better decisions? a statistical evaluation framework for experimental and observational studies. *arXiv*, 2403:v3, 2024.
- David Blackwell et al. Comparison of experiments. In *Proceedings of the second Berkeley symposium on mathematical statistics and probability*, volume 1, page 26, 1951.
- Zi-Hao Bo, Hui Qiao, Chong Tian, Yuchen Guo, Wuchao Li, Tiantian Liang, Dongxue Li, Dan Liao, Xianchun Zeng, Leilei Mei, et al. Toward human intervention-free clinical diagnosis of intracranial aneurysm via deep neural network. *Patterns*, 2(2), 2021.
- Elizabeth Bondi, Raphael Koster, Hannah Sheahan, Martin Chadwick, Yoram Bachrach, Taylan Cemgil, Ulrich Paquet, and Krishnamurthy Dvijotham. Role of human-ai interaction in selective prediction. In *Proceedings of the AAAI Conference on Artificial Intelligence*, volume 36, pages 5286–5294, 2022.
- Melanie M Boskemper, Megan L Bartlett, and Jason S McCarley. Measuring the efficiency of automation-aided performance in a simulated baggage screening task. *Human factors*, 64(6):945–961, 2022.
- Zana Bućinca, Phoebe Lin, Krzysztof Z. Gajos, and Elena L. Glassman. Proxy tasks and subjective measures can be misleading in evaluating explainable ai systems. In *Proceedings of the 25th International Conference on Intelligent User Interfaces*, IUI '20, page 454–464, New York, NY, USA, 2020. Association for Computing Machinery. ISBN 9781450371186. doi: 10.1145/3377325.3377498. URL <https://doi.org/10.1145/3377325.3377498>.
- Adrian Bussone, Simone Stumpf, and Dymrna O’Sullivan. The role of explanations on trust and reliance in clinical decision support systems. In *2015 International Conference on Healthcare Informatics*, pages 160–169, Oct 2015. doi: 10.1109/ICHI.2015.26.
- Tianqi Chen and Carlos Guestrin. Xgboost: A scalable tree boosting system. In *Proceedings of the 22nd acm sigkdd international conference on knowledge discovery and data mining*, pages 785–794, 2016.
- Yiling Chen and Bo Waggoner. Informational substitutes. In *2016 IEEE 57th Annual Symposium on Foundations of Computer Science (FOCS)*, pages 239–247. IEEE, 2016.
- Nina Corvelo Benz and Manuel Rodriguez. Human-aligned calibration for ai-assisted decision making. *Advances in Neural Information Processing Systems*, 36:14609–14636, 2023.
- Brian Dolhansky, Joanna Bitton, Ben Pfau, Jikuo Lu, Russ Howes, Menglin Wang, and Cristian Canton Ferrer. The deepfake detection challenge (dfdc) dataset. *arXiv preprint arXiv:2006.07397*, 2020.
- Julia Dressel and Hany Farid. The accuracy, fairness, and limits of predicting recidivism. *Science advances*, 4(1):eaao5580, 2018.
- Riccardo Fogliato, Alexandra Chouldechova, and Zachary Lipton. The impact of algorithmic risk assessments on human predictions and its analysis via crowdsourcing studies. *Proceedings of the ACM on Human-Computer Interaction*, 5(CSCW2):1–24, 2021.
- Drew Fudenberg, Jon Kleinberg, Annie Liang, and Sendhil Mullainathan. Measuring the completeness of economic models. *Journal of Political Economy*, 130(4):956–990, 2022.
- Ary L Goldberger, Luis AN Amaral, Leon Glass, Jeffrey M Hausdorff, Plamen Ch Ivanov, Roger G Mark, Joseph E Mietus, George B Moody, Chung-Kang Peng, and H Eugene Stanley. Physiobank, physiotoolkit, and physionet: components of a new research resource for complex physiologic signals. *circulation*, 101(23):e215–e220, 2000.

- Ben Green and Yiling Chen. Disparate interactions: An algorithm-in-the-loop analysis of fairness in risk assessments. In *Proceedings of the conference on fairness, accountability, and transparency*, pages 90–99, 2019a.
- Ben Green and Yiling Chen. The principles and limits of algorithm-in-the-loop decision making. *Proceedings of the ACM on Human-Computer Interaction*, 3(CSCW):1–24, 2019b.
- Matthew Groh, Ziv Epstein, Chaz Firestone, and Rosalind Picard. Deepfake detection by human crowds, machines, and machine-informed crowds. *Proceedings of the National Academy of Sciences*, 119(1):e2110013119, 2022.
- William M Grove, David H Zald, Boyd S Lebow, Beth E Snitz, and Chad Nelson. Clinical versus mechanical prediction: A meta-analysis. *Psychological Assessment*, 12(1):19, 2000.
- Ziyang Guo, Yifan Wu, Jason D Hartline, and Jessica Hullman. A decision theoretic framework for measuring ai reliance. In *The 2024 ACM Conference on Fairness, Accountability, and Transparency*, pages 221–236, 2024.
- Kaiming He, Xiangyu Zhang, Shaoqing Ren, and Jian Sun. Deep residual learning for image recognition. In *Proceedings of the IEEE conference on computer vision and pattern recognition*, pages 770–778, 2016.
- Paul A Heidenreich, Biykem Bozkurt, David Aguilar, Larry A Allen, Joni J Byun, Monica M Colvin, Anita Deswal, Mark H Drazner, Shannon M Dunlay, Linda R Evers, et al. 2022 aha/acc/hfsa guideline for the management of heart failure: a report of the american college of cardiology/american heart association joint committee on clinical practice guidelines. *Journal of the American College of Cardiology*, 79(17):e263–e421, 2022.
- Lunjia Hu and Yifan Wu. Predict to minimize swap regret for all payoff-bounded tasks. *arXiv preprint arXiv:2404.13503*, 2024.
- Gao Huang, Zhuang Liu, Laurens Van Der Maaten, and Kilian Q Weinberger. Densely connected convolutional networks. In *Proceedings of the IEEE conference on computer vision and pattern recognition*, pages 4700–4708, 2017.
- Jessica Hullman and Andrew Gelman. Designing for interactive exploratory data analysis requires theories of graphical inference. *Harvard Data Science Review*, 3(3):10–1162, 2021.
- Jeremy Irvin, Pranav Rajpurkar, Michael Ko, Yifan Yu, Silvana Ciurea-Ilcus, Chris Chute, Henrik Marklund, Behzad Haghighi, Robyn Ball, Katie Shpanskaya, et al. Chexpert: A large chest radiograph dataset with uncertainty labels and expert comparison. In *Proceedings of the AAAI conference on artificial intelligence*, volume 33, pages 590–597, 2019.
- Maia Jacobs, Melanie F Pradier, Thomas H McCoy Jr, Roy H Perlis, Finale Doshi-Velez, and Krzysztof Z Gajos. How machine-learning recommendations influence clinician treatment selections: the example of antidepressant selection. *Translational psychiatry*, 11(1):108, 2021.
- Alistair EW Johnson, Tom J Pollard, Seth J Berkowitz, Nathaniel R Greenbaum, Matthew P Lungren, Chih-ying Deng, Roger G Mark, and Steven Horng. MIMIC-CXR, a de-identified publicly available database of chest radiographs with free-text reports. *Scientific data*, 6(1):317, 2019.
- Alistair EW Johnson, Lucas Bulgarelli, Lu Shen, Alvin Gayles, Ayad Shammout, Steven Horng, Tom J Pollard, Sicheng Hao, Benjamin Moody, Brian Gow, et al. MIMIC-IV, a freely accessible electronic health record dataset. *Scientific data*, 10(1):1, 2023.
- Vijay Keswani, Matthew Lease, and Krishnaram Kenthapadi. Towards unbiased and accurate deferral to multiple experts. In *Proceedings of the 2021 AAAI/ACM Conference on AI, Ethics, and Society*, pages 154–165, 2021.
- Vijay Keswani, Matthew Lease, and Krishnaram Kenthapadi. Designing closed human-in-the-loop deferral pipelines. *arXiv preprint arXiv:2202.04718*, 2022.

- Bobby Kleinberg, Renato Paes Leme, Jon Schneider, and Yifeng Teng. U-calibration: Forecasting for an unknown agent. In *The Thirty Sixth Annual Conference on Learning Theory*, pages 5143–5145. PMLR, 2023.
- Jon Kleinberg, Jens Ludwig, Sendhil Mullainathan, and Ziad Obermeyer. Prediction policy problems. *American Economic Review*, 105(5):491–495, 2015.
- Jon Kleinberg, Himabindu Lakkaraju, Jure Leskovec, Jens Ludwig, and Sendhil Mullainathan. Human decisions and machine predictions. *The quarterly journal of economics*, 133(1):237–293, 2018.
- Igor Kononenko. Machine learning for medical diagnosis: history, state of the art and perspective. *Artificial Intelligence in medicine*, 23(1):89–109, 2001.
- Vivian Lai and Chenhao Tan. On human predictions with explanations and predictions of machine learning models: A case study on deception detection. In *Proceedings of the conference on fairness, accountability, and transparency*, pages 29–38, 2019.
- Himabindu Lakkaraju, Jon Kleinberg, Jure Leskovec, Jens Ludwig, and Sendhil Mullainathan. The selective labels problem: Evaluating algorithmic predictions in the presence of unobservables. In *Proceedings of the 23rd ACM SIGKDD International Conference on Knowledge Discovery and Data Mining*, pages 275–284, 2017.
- Yingkai Li, Jason D Hartline, Liren Shan, and Yifan Wu. Optimization of scoring rules. In *Proceedings of the 23rd ACM Conference on Economics and Computation*, pages 988–989, 2022.
- Zhiyuan “Jerry” Lin, Jongbin Jung, Sharad Goel, and Jennifer Skeem. The limits of human predictions of recidivism. *Science advances*, 6(7):eaaz0652, 2020.
- Ze Liu, Yutong Lin, Yue Cao, Han Hu, Yixuan Wei, Zheng Zhang, Stephen Lin, and Baining Guo. Swin transformer: Hierarchical vision transformer using shifted windows. In *Proceedings of the IEEE/CVF international conference on computer vision*, pages 10012–10022, 2021.
- Scott M Lundberg and Su-In Lee. A unified approach to interpreting model predictions. In I. Guyon, U. V. Luxburg, S. Bengio, H. Wallach, R. Fergus, S. Vishwanathan, and R. Garnett, editors, *Advances in Neural Information Processing Systems 30*, pages 4765–4774. Curran Associates, Inc., 2017.
- David Madras, Toni Pitassi, and Richard Zemel. Predict responsibly: improving fairness and accuracy by learning to defer. *Advances in neural information processing systems*, 31, 2018.
- Bryce McLaughlin and Jann Spiess. Algorithmic assistance with recommendation-dependent preferences. In *Proceedings of the 24th ACM Conference on Economics and Computation*, EC ’23, page 991, New York, NY, USA, 2023. Association for Computing Machinery. ISBN 9798400701047. doi: 10.1145/3580507.3597775. URL <https://doi.org/10.1145/3580507.3597775>.
- Paul E Meehl. *Clinical Versus Statistical Prediction: A Theoretical Analysis and a Review of the Evidence*. University of Minnesota Press, 1954.
- Hussein Mozannar, Gagan Bansal, Adam Fourney, and Eric Horvitz. When to show a suggestion? integrating human feedback in ai-assisted programming. In *Proceedings of the AAAI Conference on Artificial Intelligence*, volume 38, pages 10137–10144, 2024a.
- Hussein Mozannar, Jimin Lee, Dennis Wei, Prasanna Sattigeri, Subhro Das, and David Sontag. Effective human-ai teams via learned natural language rules and onboarding. *Advances in Neural Information Processing Systems*, 36, 2024b.
- Christian Mueller, Kenneth McDonald, Rudolf A de Boer, Alan Maisel, John GF Cleland, Nikola Kozhuharov, Andrew JS Coats, Marco Metra, Alexandre Mebazaa, Frank Ruschitzka, et al. Heart failure association of the european society of cardiology practical guidance on the use of natriuretic peptide concentrations. *European journal of heart failure*, 21(6):715–731, 2019.
- Sendhil Mullainathan and Ziad Obermeyer. Diagnosing physician error: A machine learning approach to low-value health care. *The Quarterly Journal of Economics*, 137(2):679–727, 2022.

- Nastaran Okati, Abir De, and Manuel Rodriguez. Differentiable learning under triage. *Advances in Neural Information Processing Systems*, 34:9140–9151, 2021.
- Samir Passi and Mihaela Vorvoreanu. Overreliance on ai literature review. *Microsoft Research*, 339:340, 2022.
- Maithra Raghu, Katy Blumer, Greg Corrado, Jon Kleinberg, Ziad Obermeyer, and Sendhil Mullainathan. The algorithmic automation problem: Prediction, triage, and human effort. *arXiv preprint arXiv:1903.12220*, 2019.
- Pranav Rajpurkar, Jeremy Irvin, Robyn L Ball, Kaylie Zhu, Brandon Yang, Hershel Mehta, Tony Duan, Daisy Ding, Aarti Bagul, Curtis P Langlotz, et al. Deep learning for chest radiograph diagnosis: A retrospective comparison of the chexnext algorithm to practicing radiologists. *PLoS medicine*, 15(11):e1002686, 2018.
- Ashesh Rambachan. Identifying prediction mistakes in observational data. *The Quarterly Journal of Economics*, page qjae013, 2024.
- Charvi Rastogi, Liu Leqi, Kenneth Holstein, and Hoda Heidari. A taxonomy of human and ml strengths in decision-making to investigate human-ml complementarity. In *Proceedings of the AAAI Conference on Human Computation and Crowdsourcing*, volume 11, pages 127–139, 2023.
- Max Schemmer, Patrick Hemmer, Maximilian Nitsche, Niklas Köhl, and Michael Vössing. A meta-analysis of the utility of explainable artificial intelligence in human-ai decision-making. In *Proceedings of the 2022 AAAI/ACM Conference on AI, Ethics, and Society*, pages 617–626, 2022.
- Lloyd S Shapley. A value for n-person games. *Contributions to the Theory of Games*, 2, 1953.
- Advik Shreekumar. X-raying experts: Decomposing predictable mistakes in radiology. 2025.
- Christian Szegedy, Vincent Vanhoucke, Sergey Ioffe, Jon Shlens, and Zbigniew Wojna. Rethinking the inception architecture for computer vision. In *Proceedings of the IEEE conference on computer vision and pattern recognition*, pages 2818–2826, 2016.
- Yu-Xing Tang, You-Bao Tang, Yifan Peng, Ke Yan, Mohammadhadi Bagheri, Bernadette A Redd, Catherine J Brandon, Zhiyong Lu, Mei Han, Jing Xiao, et al. Automated abnormality classification of chest radiographs using deep convolutional neural networks. *NPJ digital medicine*, 3(1):70, 2020.
- Michelle Vaccaro and Jim Waldo. The effects of mixing machine learning and human judgment. *Communications of the ACM*, 62(11):104–110, 2019.
- Michelle Vaccaro, Abdullah Almaatouq, and Thomas Malone. When combinations of humans and ai are useful: A systematic review and meta-analysis. *Nature Human Behaviour*, pages 1–11, 2024.
- Bryan Wilder, Eric Horvitz, and Ece Kamar. Learning to complement humans. In *Proceedings of the Twenty-Ninth International Conference on International Joint Conferences on Artificial Intelligence*, pages 1526–1533, 2021.
- Yifan Wu, Ziyang Guo, Michalis Mamakos, Jason Hartline, and Jessica Hullman. The rational agent benchmark for data visualization. *IEEE transactions on visualization and computer graphics*, 2023.
- Kaipeng Zhang, Zhanpeng Zhang, Zhifeng Li, and Yu Qiao. Joint face detection and alignment using multitask cascaded convolutional networks. *IEEE signal processing letters*, 23(10):1499–1503, 2016.

A The Combinatorial Nature of the Value of Signals

We model the information value of a single signal over the existing information in agent decisions. When decision-makers are provided with multiple signals, they might use them in combination. Therefore, our definition of information value in Definition 3.2 may overlook the signals' value in combination with other signals. Signals can be complemented [Chen and Waggoner, 2016], i.e, they contain no information value by themselves but a considerable value when combined with other signals. For example, two signals Σ_1 and Σ_2 ight be uniformly random bits and the state $\omega = \Sigma_1 \oplus \Sigma_2$, the XOR of Σ_1 and Σ_2 . In this case, neither of the signals offers information value on its own, but knowing both leads to the maximum payoff. To consider this complementation between signals, we use the Shapley value ϕ [Shapley, 1953] to interpret the contribution to information gain of each basic signal. The Shapley value calculates the average of the marginal contribution of a basic signal Σ_i in every combination of signals.

$$\phi(\Sigma_i) = \frac{1}{n} \sum_{V \subseteq \{V_1, \dots, V_n\} / \{\Sigma_i\}} \binom{n-1}{|V|}^{-1} (\text{ACIV}(V \cup \{\Sigma_i\}; D^b) - \text{ACIV}(V; D^b)) \quad (10)$$

The Shapley value suggests how much information value of the basic signal is unexploited by the human decision-maker on average in all combinations.

The following algorithm provides a polynomial-time approximation of the Shapley value of ACIV. Under the assumption of submodularity, it orders the signals the same as the Shapley value.

Algorithm 1 Greedy algorithm for marginal gain of ACIV

```

1:  $V^* = \{D^b\}$ 
2:  $\Phi^* = \{\}$ 
3: for  $i = 1$  to  $n$  do
4:    $\phi'_j = \text{ACIV}(\Sigma_j; V^*)$  for each  $j$ 
5:    $j^* = \arg \max_j$  s.t.  $\Sigma_j \notin V^*$   $\phi'_j$ 
6:    $\phi_{j^*} = \max_j$  s.t.  $\Sigma_j \notin V^*$   $\phi'_j$ 
7:   add  $\Sigma_{j^*}$  to  $V^*$ 
8:   add  $\phi_{j^*}$  to  $\Phi^*$ 
9: end for
10: output  $\phi_{j^*}$ 

```

B Embeddings for High-dimensional Signals in Decision Problem

Suppose the data-generating process is estimated from a set of observations $\{(\omega_i, v_i)\}_{i=1}^T$, i.e.,

$$\hat{\pi}(\omega, v) = \frac{1}{T} \sum_{i=1}^T \mathbb{1}_{\omega=\omega_i} \cdot \mathbb{1}_{v=v_i} \quad (11)$$

In this case, the sample size T that is required to get a good estimate of DGP is the exponential of the number of dimensions of the signal v . The high-dimensional signals, such as images and text, that are usual in human-AI decision problems are not computationally feasible to be quantified under our framework. We propose a systematic procedure to pick the optimal reduction model to represent the high-dimensional signal space in a low-dimensional embedding space.

The optimal reduction model and its generated embeddings should fulfill two properties. First, the generated signals should be as informative as possible for the decision task, such that they maintain the maximum information value contained in the original signals. Second, the derived DGP that is implied by the embedding signals should be feasible to be estimated from the observed dataset. We quantify the above objectives by a framework based on Train/Test split.

Algorithm 2 Embedding high-dimensional signals in decision problems

- 1: Input: Observed dataset $\{(\omega_i, v_i)\}_{i=1}^T$, Candidate model generator C .
 - 2: $R^* = 0$
 - 3: Split the dataset into a training set and a testing set.
 - 4: **repeat**
 - 5: Generate a candidate model c from C .
 - 6: Generate embedding $v_i^c = c(v_i)$ on each data point of both sets.
 - 7: Estimate the DGP $\hat{\pi}$ implied by the new signals v_i^c by Equation (11).
 - 8: Calculate rational decision rule:

$$d^r(v^c) = \arg \max_{d \in \mathbf{D}} \mathbf{E}_{\omega \sim \pi(\omega|v^c)}[S(d, \omega)].$$
 - 9: Calculate training performance $R_{training} = \mathbf{E}_{(v^c, \omega) \sim training_set}[S(d^r(v^c), \omega)]$.
 - 10: Calculate testing performance $R_{testing} = \mathbf{E}_{(v^c, \omega) \sim testing_set}[S(d^r(v^c), \omega)]$.
 - 11: **if** $R_{training} - R_{testing} > \tau$ **then**
 - 12: go to step 4.
 - 13: **end if**
 - 14: **if** $R^* < R_{training}$ **then**
 - 15: $c^* = c$.
 - 16: $R^* = R_{training}$.
 - 17: **end if**
 - 18: **until** no more new candidate model in C or R^* converges
 - 19: Output: c^*
-

The threshold τ represents the tolerance in the exchangeability between the signal-state tuples in the training set and the testing set. When the candidate model space is infinite, the optimal reduction model can still be found if the candidate space is a lattice that is defined by the informativeness of their generated embeddings, e.g., a class of embedding models with different parameter p in the dropout layer.

C Robustness Analysis in Experiment I

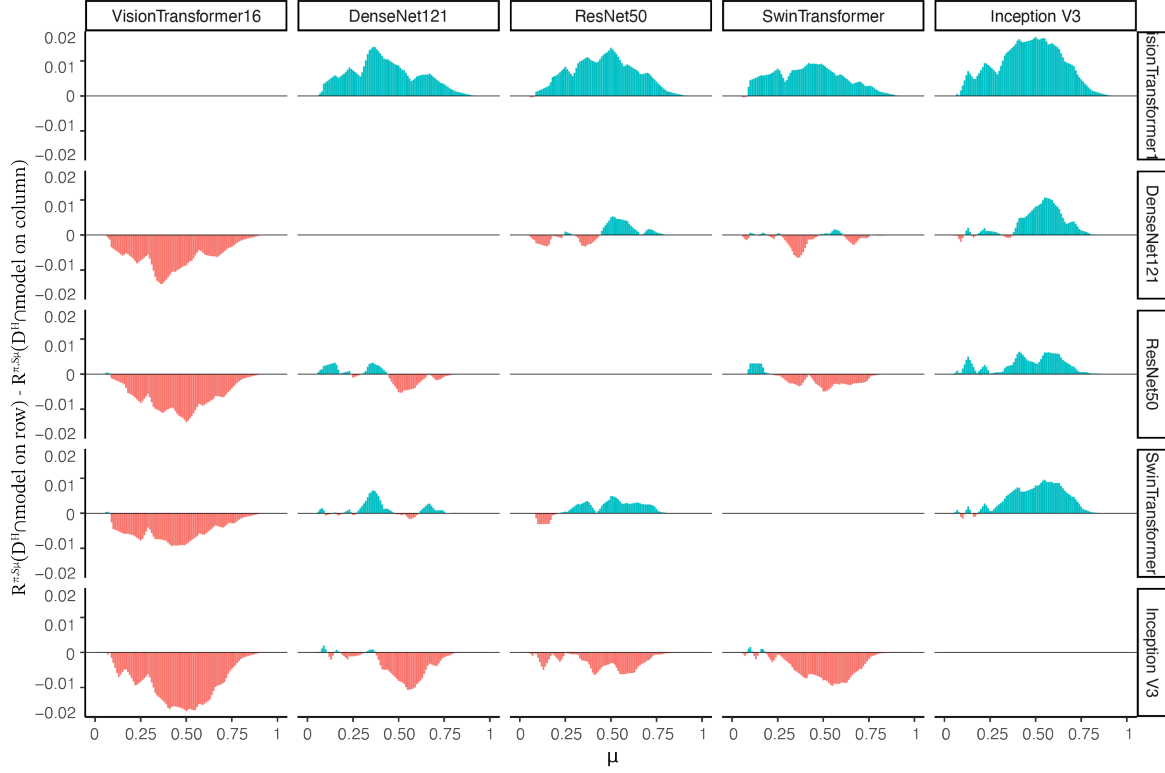
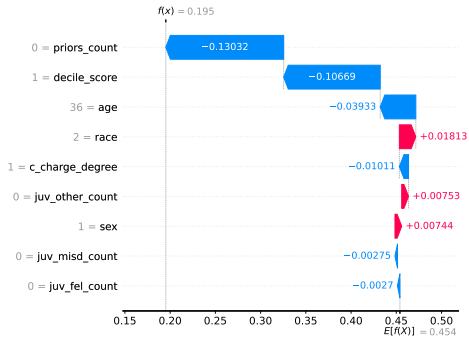
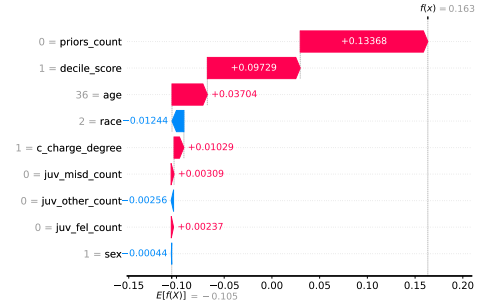


Figure 4: Robust analysis for experiment I on all V-shaped payoff functions. The kink μ is shown on the x -axis. Each subplot displays the difference between the ACIV on the row model over human decisions and the ACIV on the column model over human decisions. A positive value (colored in blue) at μ indicates the model on the row contains more informative than the model on the column under the evaluation of V-shaped scoring rule with kink μ . The subplots are symmetric along the diagonal, e.g., (1, 2) subplot and (2, 1) subplot display the same distribution with opposite signs.

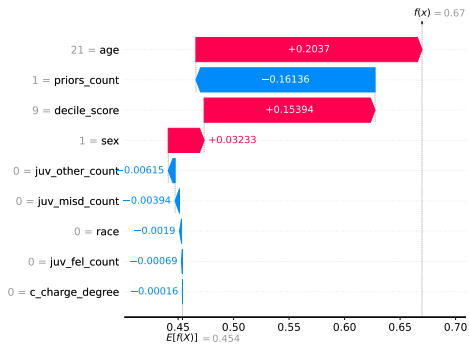
D More examples of ILIV-SHAP



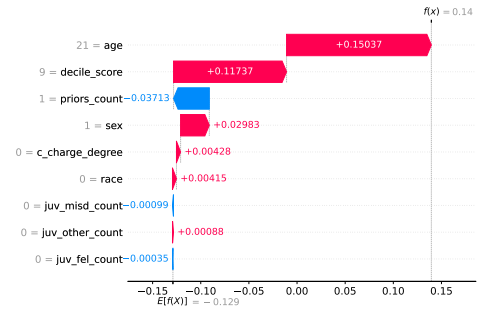
(a) SHAP on instance 0



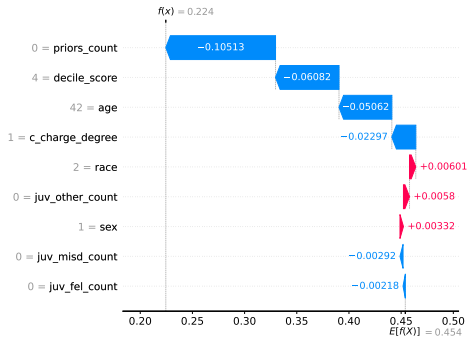
(b) ILIV-SHAP on instance 0



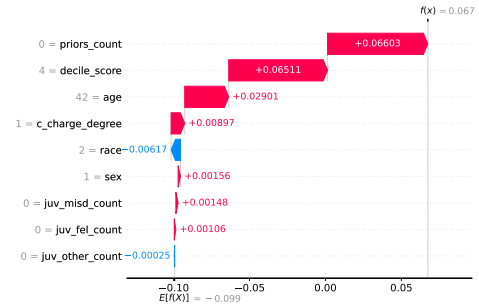
(a) SHAP on instance 1



(b) ILIV-SHAP on instance 1



(a) SHAP on instance 2



(b) ILIV-SHAP on instance 2